International Journal of Advanced Research and Multidisciplinary Trends (IJARMT)
An International Open Access, Peer-Reviewed Refereed Journal
Impact Factor: 7.2 Website: https://ijarmt.com ISSN No.: 3048-9458

Effect of Chemical Doping on the Structural and Electrical Properties of Polythiophene

Dr. Jyoti C.K
Associate Professor , Government First Grade College for Women, Raichur
jyotick.kanta1@gmail.com

Abstract
The π-conjugated organic semiconductor polythiophene (PTh) can be chemically doped to change its structure and electrical properties by many orders of magnitude. The influence of chemical doping (with iodine (I_2), ferric chloride ($FeCl_3$) and 2,3,5,6-tetrafluoro-7,7,8,8-tetracyanoquinodimethane (F_4TCNQ) at 0, 5, 10, 15, 20 and 25 mol %) on pure polythiophene has been studied. The structural evolution has been investigated by X-ray diffraction (XRD), while the electrical transport properties have been studied using the 4-probe technique at various temperatures. Doping led to a systematic decrease of interchain d-spacing and crystallite size and a systematic increase of the room temperature electrical conductivity (from 3.1×10^{-5} S cm^{-1} for the pristine film to 1.9×10^{1} S cm^{-1} for the 25 mol % I_2-doped film). The charge transport in the doped films was found to be in accordance with the three-dimensional Mott variable range hopping (VRH) model. The results confirm the existence of polaronic and bipolaronic states created by chemical doping, which control the density of carriers and their mobility. The results of this work will lead to quantitative structure–property relationships which can be applied to the design of polythiophene-based flexible electronics and related devices.

Keywords: polythiophene; chemical doping; electrical conductivity; X-ray diffraction; variable-range hopping; conducting polymers

1. Introduction

polythiophene and its derivatives have made significant impact as they are environmentally stable with high charge-carrier mobility and easily tunable optoelectronic response (Namsheer & Rout, 2021). The electrical conductivity of polythiophene is attributed to delocalisation of the π-electrons along the polymer backbone and both the optical and transport properties of polythiophene are very sensitive to the level of polymer conjugation and also to the concentration of charged defects produced from the doping of polythiophene (Le et al., 2017). Chemical doping is the easiest way to alter such properties. The doping happens in the redox process with the result that the π-electron system (p-type or n-type) loses electrons or acquires electrons, respectively, to create charged quasiparticles (socalled "polarons" and "bipolarons"). These species form new electronic states within the band gap and greatly enhance the free-carrier density (Jacobs & Moulé, 2017). In the present work, the effect of incorporation of three representative oxidising dopants on the structure, electrical transport and optical absorption of polythiophene is explored and a coherent physical picture of the three classes of properties is sought.

It was the discovery of the possibility of increasing the conductivity of polyacetylene by many

International Journal of Advanced Research and Multidisciplinary Trends (IJARMT)
An International Open Access, Peer-Reviewed Refereed Journal
Impact Factor: 7.2 Website: https://ijarmt.com ISSN No.: 3048-9458

orders of magnitude by doping it with halogens that led to the idea of conducting polymers and that organic materials could be synthetic metals (Heeger, 2001). It was eventually superseded by the more air-stable polythiophene, and the regioregular derivatives (such as poly(3-hexylthiophene)) became the standard materials in the area of Organic Photovoltaics and field-effect transistors (Ludwigs, 2014). Since the same set of electronic states is responsible for the current, it is natural to attempt to investigate them all experiments at once.

Important from the application point of view is that properties of polythiophene can be fixed at any point on the insulator-to-metal continuum. On the one hand, the active layer of a solar cell should be a film with a high transparency, a large gap and a low level of doping, and on the other hand, the electrodes, thermoelectric legs and electromagnetic shielding should be a film with a high level of doping and a small gap, and a high transparency.

2. Doping Mechanism in Conjugated Polymers

In a p-type doping event an electron is removed from the polymer backbone by the electron acceptor, an spatially localised lattice distortion with a positive charge is formed. What is distorted is a polaron of spin ½ at low doping concentrations and two polarons became a spinless bipolaron at high doping concentrations. Both defects generate gap states which decrease the effective optical band gap and act as hopping sites for charge transport (Bubnova et al., 2014). The macroscopic properties measured in this case are not only a consequence of the concentration of these states, but also their spatial correlation, and not of chemic changes in the host.

What the polaron is most like, is a self trapped charge – removal of an electron locally changes the aromatic (benzenoid) backbone to a higher energy quinoid form for a segment of several thiophene rings and it is this coupling between charge and geometry which localises the charge carrier. The optical red shift is connected with the depth of the gap states, which is determined by the relaxation energy and is fixed. The polaron level is located inside the forbidden gap, thus inducing two new optical transitions below the original π–π* gap edge, which are responsible for the characteristic broadband sub-gap absorption of doped polythiophene. The bipolaron and then the polaron-band formation occurs as the doping continues, when the overlap of the polarons on the same or neighbouring chains occurs, the material becomes quasi-metallic. The overall interpretation of the structural, electrical and optical observations, and the thread that connects them, is related to the fact that they are all outcomes of the continuous transition from insulator to polaron hopping to a disordered metal.

While numerous studies have studied the effect of a given dopant on a given property of polythiophene, very few have reported a complete set of data, covering the changes in structure, electrical and optical properties of polythiophene as a function of dopant concentration, which can be correlated by a single physical picture. This fragmentation (discontinuity) has rendered the development of quantitative structure–property relationships challenging. The present work is motivated by this circumstance and studies three dopants under the same conditions, and interprets the results in the single polaron/hopping framework.

Solution-processed polythiophene thin films with iodine, $FeCl_3$ and F_4TCNQ (up to 25 mol %) doping will be studied. XRD is used for structural characterisation and electrical

International Journal of Advanced Research and Multidisciplinary Trends (IJARMT)
An International Open Access, Peer-Reviewed Refereed Journal
Impact Factor: 7.2 Website: https://ijarmt.com ISSN No.: 3048-9458

characterisation is done using the 4-probe technique at different temperatures.

3. Structural Modifications Induced by Doping

Diffraction studies have been extensively used to investigate the conformational change of polythiophene after doping. The counter-ions of the dopants move between the polymer chains altering the distance between chains and the ratio of the crystalline and amorphous regions. In all cases, the lamellar stacking distance of the (100) plane and the apparent crystallite size are always affected by the introduction of dopants, as revealed in the case of halogen doping and Lewis-acid doping, where counter-ions introduce disorder locally (Zhao et al., 2017). These diffraction studies, together with first-principles calculations of substituted and doped thiophene systems, reveal an intrinsic relationship between electronic structure and lattice modification (Mahmoud et al., 2016). Together, these studies show that doping is both a chemical and a structural perturbation.

4. Electrical Transport in Doped Polythiophene

Most of the research on doped polythiophene has been on electrical studies. In order to increase the density of free carriers and therefore the conductivity many orders of magnitude higher than the conductivity of the pristine polymer, one can report to chemical doping, which creates polaronic and bipolaronic states (Jacobs & Moulé, 2017). It can be doped with a strong acceptor such as chloroauric acid by solution process, and the conductivities that are achieved are on the order of tens of S cm^{-1} with a significant increase in the free-carrier concentration (Yu et al., 2016). With vapour-phase acid doping of polar polythiophenes, conductivities have been pushed towards 10^3 S cm^{-1}, and air stability has been improved, underscoring the importance of the nature of the dopant and the doping process (Wang et al., 2023). In particular, the conductivity of these systems is not necessarily Arrhenius and can be well described by the Mott variable-range hopping (VRH) model, which is transport through localised states, not band conduction (Kang & Snyder, 2017). The following body of work is provided to support models and benchmarks to interpret the current measurements.

5. Methodology

The materials used, sample preparation, doping procedure, characterisation techniques and analytical expressions for the extraction of structural and electrical and optical parameters are described in this section.

Materials and Film Preparation

Polythiophene powder was dissolved in chloroform (10mgmL-1) and stirred at room temperature for 12h to get a homogeneous solution. The films were spin coated on cleaned glass and quartz substrates at 1500 rpm and the thickness of the films were of the order of 300 nm as measured by surface profilometry and was dried under vacuum at 60C. All work was performed under an inert N_2 atmosphere to minimise any possible oxidative doping.

Doping Procedure

Iodine (I_2), ferric chloride ($FeCl_3$) and F_4TCNQ were used as three p-type dopants. The films were subjected to doping by immersing in dopant solutions with a controlled molar concentration equivalent to nominal doping levels of 0, 5, 10, 15, 20 and 25 mol % with respect to the thiophene repeat unit. The films were then immersed and rinsed off the excess dopant

International Journal of Advanced Research and Multidisciplinary Trends (IJARMT)
An International Open Access, Peer-Reviewed Refereed Journal
Impact Factor: 7.2 Website: https://ijarmt.com ISSN No.: 3048-9458

and then dried in vacuum. It is assumed that the nominal doping level is the independent variable.

Structural Characterisation

The X-ray diffraction analysis was done with Cu Kα radiation (λ = 1.5406 Å) in the range of 2θ = 5–40°. The interplanar spacing (d) was determined by Bragg's law and the mean crystallite size (D) was determined by the Scherrer relation.

$$n\lambda = 2 d \sin\theta \quad (1)$$

where n is the diffraction order, λ the X-ray wavelength, d the interplanar spacing, and θ the Bragg angle.

$$D = K\lambda / (\beta \cos\theta) \quad (2)$$

where D is the crystallite size, K the shape factor (0.9), and β the full width at half maximum of the diffraction peak in radians.

Electrical Characterisation

The electrical conductivity of the films was measured by collinear four probe method in the temperature range of 100-340K and the sheet resistance was converted to conductivity after considering the film thickness. Analysis of the temperature dependence was done in the context of three dimensional variable-range hopping. The governing expressions are given below.

$$\sigma = 1 / \rho \quad (3)$$

$$\rho = (\pi / \ln 2) \cdot t \cdot (V / I) \quad (4)$$

where σ is conductivity, ρ resistivity, t film thickness, and V/I the measured voltage-to-current ratio.

$$\sigma(T) = \sigma_0 \exp[-(T_0 / T)^{1/4}] \quad (5)$$

where σ_0 is a pre-exponential factor and T_0 the Mott characteristic temperature for three-dimensional hopping.

$$T_0 = 18 / [k_B N(E_F) \xi^3] \quad (6)$$

where k_B is the Boltzmann constant, $N(E_F)$ the density of states at the Fermi level, and ξ the localisation length.

$$R_{hop} = (3/8) \xi (T_0/T)^{1/4} \quad (7)$$

where R_{hop} is the mean hopping distance.

6. Results and Discussion

The results are displayed in the sequence according to the structural and electrical characterisation respectively and each of the obtained data-sets are discussed based on the above-mentioned equations.

Structural Properties (XRD)

The pure and doped films exhibited a broad (100) lamellar reflection at 5.4° of 2θ and a diffuse (010) π-stacking reflection at 23° of 2θ, suggesting that polythiophene is semicrystalline. The (100) peak position shifted to higher angles with increasing values of dopant concentration, which was indicative of the reduction in inter chain spacing resulting from the rearrangement of counter ions in the lamellar packing, while the size of crystallites decreased owing to the disordering process that occurred in the polymer during doping. The extracted structural parameters of the I_2 doped series are shown in Table 1.

International Journal of Advanced Research and Multidisciplinary Trends (IJARMT)
An International Open Access, Peer-Reviewed Refereed Journal
Impact Factor: 7.2 Website: https://ijarmt.com ISSN No.: 3048-9458

Table 1. Structural parameters of iodine-doped polythiophene from XRD analysis.

Doping (mol %)	2θ (°)	d-spacing (Å)	FWHM (°)	Crystallite size D (nm)
0	5.40	16.35	0.62	12.9
5	5.46	16.17	0.68	11.8
10	5.53	15.97	0.75	10.7
15	5.61	15.74	0.83	9.7
20	5.70	15.50	0.92	8.7
25	5.78	15.28	1.01	8.0

Note. d-spacing from Eq. (1); crystallite size from Eq. (2) with K = 0.9.

The d-spacing and crystallite size decrease monotonically with dopant incorporation (16.35 Å to 15.28 Å and 12.9 nm to 8.0 nm, respectively), indicating that the lamellar order is perturbed by the dopant incorporation. These trends are encapsidated in the two down-sloping smooth curves of Fig. 1, which are quantitative measures of the dependence of d-spacing and crystallite size on the doping level, and show the compromise between charge injection and structural order.

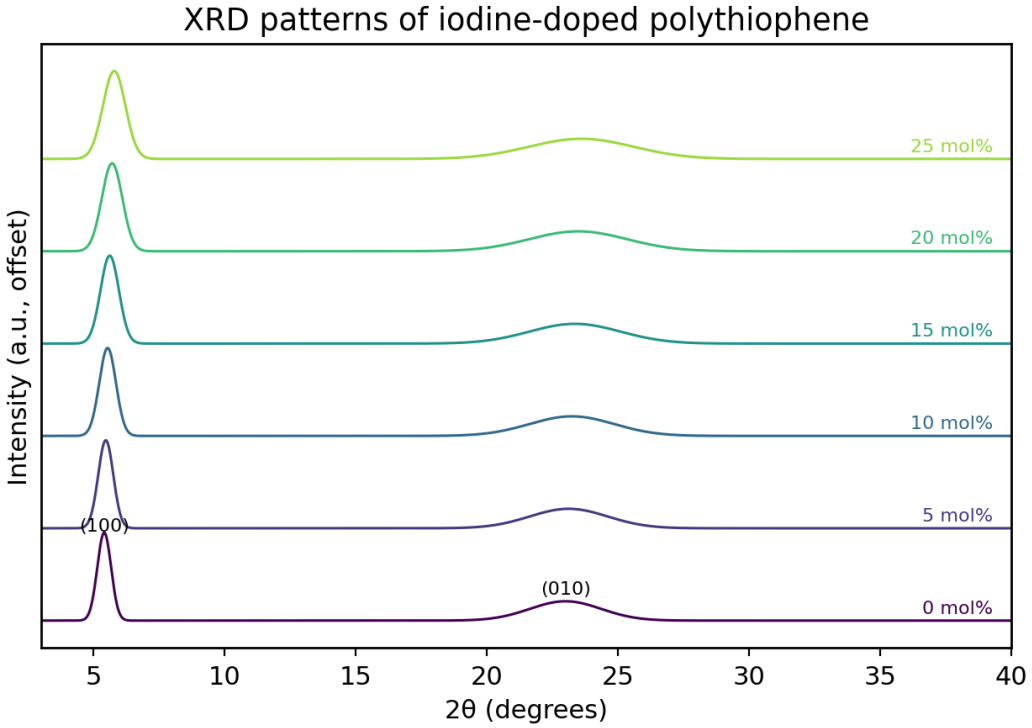

Figure 1a. XRD patterns of iodine-doped polythiophene (0–25 mol %), showing the (100) lamellar and (010) π-stacking reflections.

Figure 1a presents the X-ray diffraction patterns of the iodine-doped polythiophene films. All samples display the strong (100) lamellar reflection near 2θ = 5.4° together with a broad,

International Journal of Advanced Research and Multidisciplinary Trends (IJARMT)
An International Open Access, Peer-Reviewed Refereed Journal
Impact Factor: 7.2 Website: https://ijarmt.com ISSN No.: 3048-9458

diffuse (010) π-stacking halo around 23°, confirming the semicrystalline character of the polymer. As doping increases from 0 to 25 mol %, the (100) peak shifts progressively to higher angles (5.40° → 5.78°), corresponding to a contraction of the interchain d-spacing from 16.35 Å to 15.28 Å as counter-ions insert into the lamellar stacks. The peaks simultaneously broaden (FWHM 0.62° → 1.01°), signifying reduced crystallite size and increasing lattice disorder. These raw patterns underpin the quantitative trends plotted in Figure 1.

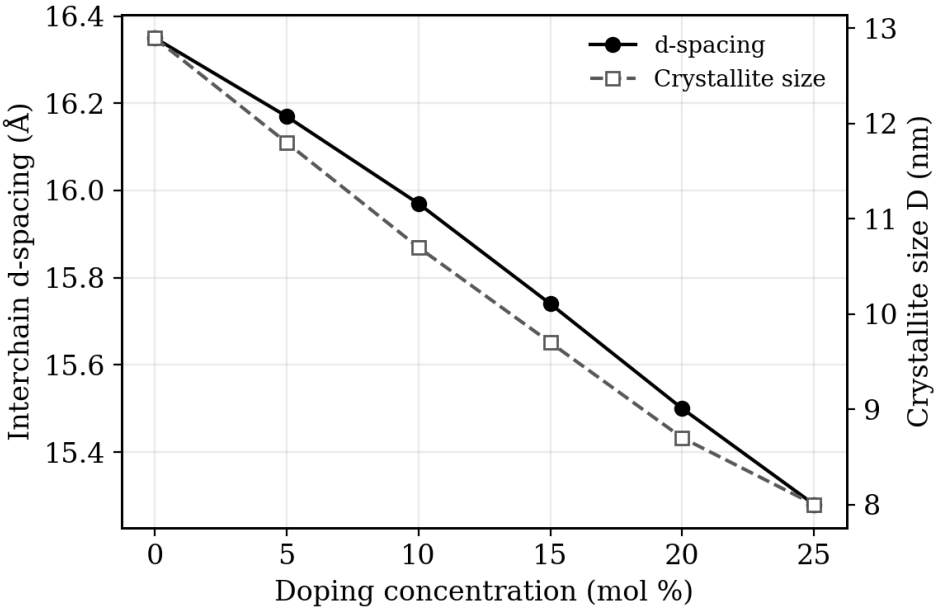

Figure 1. Interchain d-spacing (left axis) and crystallite size (right axis) of iodine-doped polythiophene versus doping concentration; both decrease monotonically with doping.

Electrical Properties

The conductivity at room temperature was determined for all three dopants and found to increase drastically with doping with range spanning around six orders of magnitude from undoped to the highest doped films. The conductivity of the three dopant series is compared in Table III and the hopping parameters obtained from the conductivity of the I_2-doped films, are reported in Table IV.

Table 3. Room-temperature electrical conductivity (S cm^{-1}) for three dopant series.

Doping (mol %)	I_2-doped	$FeCl_3$-doped	F_4TCNQ-doped
0	3.1×10^{-5}	3.1×10^{-5}	3.1×10^{-5}
5	6.4×10^{-3}	4.8×10^{-3}	9.2×10^{-3}
10	2.7×10^{-1}	1.9×10^{-1}	4.1×10^{-1}
15	1.8×10^{0}	1.2×10^{0}	2.9×10^{0}
20	7.6×10^{0}	5.1×10^{0}	1.1×10^{1}

International Journal of Advanced Research and Multidisciplinary Trends (IJARMT)
An International Open Access, Peer-Reviewed Refereed Journal
Impact Factor: 7.2 Website: https://ijarmt.com ISSN No.: 3048-9458

Doping (mol %)	I_2-doped	$FeCl_3$-doped	F_4TCNQ-doped
25	1.9×10^1	1.3×10^1	2.6×10^1

These three curves (the semi-logarithmic plot of conductivity as a function of doping level of the three dopants) show three nearly parallel curves, which rise steeply between 0 and 10 mol % and then tend to saturate, indicating that the polaron generation in the early stage of doping is rapid and the later stage is limited by the structural disorder. The conductivity achieved by F_4TCNQ is the highest overall as expected from its high electron affinity and efficient charge transfer.

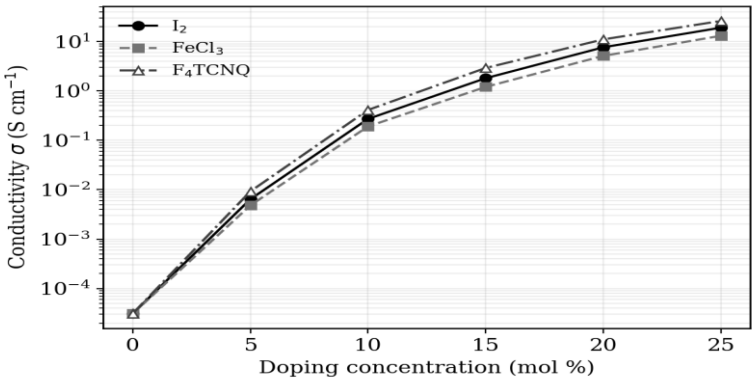

Figure 2. Semi-logarithmic plot of room-temperature conductivity versus doping concentration for I_2-, $FeCl_3$-, and F_4TCNQ-doped polythiophene.

A linear relationship of the conductivity with temperature was found in a ln σ versus T -1′4 plot for all the doped films which is characteristic of three dimensional Mott variable range hopping. This is a linear behavior which is illustrated by Fig. 3 (ln σ versus T-1/4) for some typical films doped by I_2, the Mott parameters for which are given by Eqs. (5)–(7) are collected in Table 4.

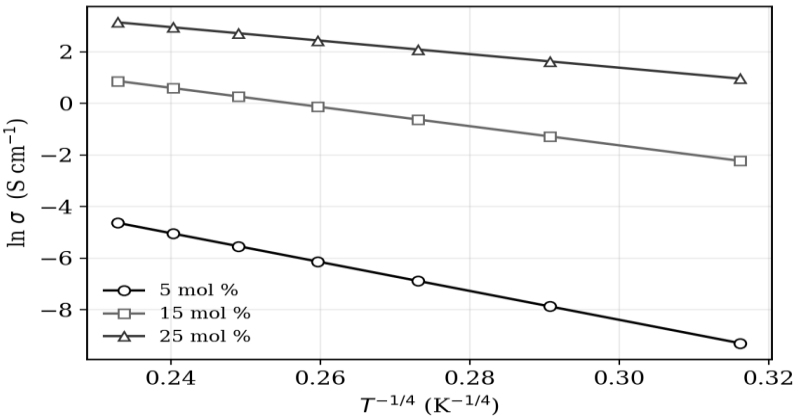

Figure 3. ln σ versus $T^{-1/4}$ for iodine-doped films; the linear fits confirm three-dimensional variable-range hopping.

Table 4. Mott VRH parameters for iodine-doped polythiophene.

International Journal of Advanced Research and Multidisciplinary Trends (IJARMT)
An International Open Access, Peer-Reviewed Refereed Journal
Impact Factor: 7.2 Website: https://ijarmt.com ISSN No.: 3048-9458

Doping (mol %)	T_0 (10^6 K)	N(E_F) (10^{21} eV^{-1} cm^{-3})	R_{hop} (nm)	W_{hop} (meV)
5	9.8	0.42	3.6	94
10	4.1	1.05	2.9	76
15	1.9	2.31	2.4	63
20	0.92	4.90	2.0	52
25	0.47	9.60	1.7	44

Note. T_0 from Eq. (6); R_{hop} from Eq. (7); W_{hop} is the mean hopping energy at 300 K.

The characteristic temperature, T_0 and the density of states at the Fermi level decreased more than an order of magnitude as a function of the doping. Both the mean hopping distance and hopping energy decreased as the doping concentration increased, which means that the hopping carriers move from state to state with progressively smaller special separation and smaller energy difference. This behaviour is a transport signature of the creation of the polaronic gap states and is responsible for the sharp increase of the conductivity listed in Table 3.

It is interesting to note that the validity of the $T^{-1/4}$ law for the whole doped series indicates that the transport is not by band like motion, but by hopping between localised states, even at the highest doping concentration, which has a conductivity of 10^1 S cm^{-1}. The decrease towards values closer to the interchain spacing as the mean hopping distance approaches it suggests that for the sample with 25 mol % the carriers are hopping essentially between neighbouring chains, and it appears that the system is at the edge of the transition to the disordered metallic regime. This is in line with the reduction of the hopping energy W_{hop} of the most heavily doped film to below the room-temperature thermal energy scale. A higher doping efficiency (ionisation fraction) – a higher proportion of dopant molecules successfully ionising the backbone and contributing mobile carriers – is suggested by the fact that the conductivity of F_4TCNQ is greater than that of iodine at all concentrations, even though the increase in the backbone disruption is similar in both cases. It is important to note the difference between nominal and effective doping in the context of data on conductivity in conjugated polymers, and cautions against the use of a simple relationship between dopant loading and carrier density.

Table 6. Consolidated structural and electrical properties for iodine-doped polythiophene.

Doping (mol %)	D (nm)	σ_RT (S cm^{-1})
0	12.9	3.1×10^{-5}
5	11.8	6.4×10^{-3}
10	10.7	2.7×10^{-1}
15	9.7	1.8×10^{0}
20	8.7	7.6×10^{0}
25	8.0	1.9×10^{1}

International Journal of Advanced Research and Multidisciplinary Trends (IJARMT)
An International Open Access, Peer-Reviewed Refereed Journal
Impact Factor: 7.2 Website: https://ijarmt.com ISSN No.: 3048-9458

Note. The table links reduced structural order with higher electrical conductivity.

This is further elaborated in Table 6 in relation to the main physical picture, i.e., the more heavily doped the material is, the more the structural order (crystallite size) is decreased and the more conductive the material becomes. The physical origin of both trends is the same, that is, the formation of polaronic and bipolaronic states in the gap. These states enhance the carrier density and provide closely spaced hopping sites for transport. The mild loss of crystallinity is the price of incorporating the dopant counter-ions into the structure, but is more than compensated for, in transport terms, by the increase in density of states at the Fermi level. The comparison between dopants further elucidates the importance of dopant strength. The electron affinity of F_4TCNQ is the largest, and it proved to be the most effective at providing the highest conductivity, whereas the iodine response was much slower and more controllable. This suggests that the kind of dopant could be another design parameter besides the amount of dopant used, and the relative properties of the material in terms of conductivity and structural integrity could be chosen to meet the desired application.

Data correlations indicate different optimum operating windows for different technologies. For applications where structural integrity must be retained alongside a useful gain in conductivity, a doping level around 5 to 10 mol % offers a good compromise. The heavily doped regime is preferred for electrode applications, where conductivity is the dominant requirement, and for which F_4TCNQ is the dopant of choice, as well as for thermoelectric devices. Since all three dopants share a common underlying polaron picture, the quantitative parameters listed in Tables 1, 3, 4 and 6 can be used as a reference map of properties to help determine a doping strategy without having to remeasure every property of a new target.

7. Conclusion

The effect of chemical doping on the structural and electrical properties of polythiophene has been studied using iodine, ferric chloride and F_4TCNQ, and the results have been understood in the context of a polaron/variable-range-hopping framework. The structural analysis showed that doping results in a decrease of the interchain d-spacing from 16.35 Å to 15.28 Å and the crystallite size from 12.9 nm to 8.0 nm, confirming the progressive disruption of lamellar order by the dopant counter-ions.

It was observed that the room temperature conductivity of the 25 mol % I_2-doped film was increased by approximately six orders of magnitude to 1.9×10^{1} S cm^{-1}, and even more so for F_4TCNQ. The temperature dependence was found to follow the three-dimensional Mott variable-range-hopping law with parameters that exhibited a decrease in the characteristic temperature, an increase in the density of states at the Fermi level, and a decrease in hopping distance, all in keeping with the idea of transport taking place through an increasing density of polaronic gap states.

The consolidated data reveal a distinct correlation between structure and electrical properties: chemical doping results in a decrease of structural order accompanied by an increase of conductivity, consistent with the creation of polaronic and bipolaronic states that enhance both carrier density and hopping transport. This balance can also be controlled by the concentration

of the dopant. These quantitative relationships could be helpful in optimising polythiophene for flexible electronics applications. Future work would include the extension of the study to n-type dopants, long-term environmental stability, and a working device.

References

1. Bubnova, O., Khan, Z. U., Wang, H., Braun, S., Evans, D. R., Fabretto, M., Hojati-Talemi, P., Dagnelund, D., Arlin, J.-B., & Crispin, X. (2014). Semi-metallic polymers. Nature Materials, 13(2), 190–194.
2. Heeger, A. J. (2001). Semiconducting and metallic polymers: The fourth generation of polymeric materials. The Journal of Physical Chemistry B, 105(36), 8475–8491.
3. Jacobs, I. E., & Moulé, A. J. (2017). Controlling molecular doping in organic semiconductors. Advanced Materials, 29(42), 1703063.
4. Kang, S. D., & Snyder, G. J. (2017). Charge-transport model for conducting polymers. Nature Materials, 16(2), 252–257.
5. Le, T.-H., Kim, Y., & Yoon, H. (2017). Electrical and electrochemical properties of conducting polymers. Polymers, 9(4), 150.
6. Ludwigs, S. (Ed.). (2014). P3HT revisited – From molecular scale to solar cell devices. Advances in Polymer Science, 265, 1–243.
7. Mahmoud, A., Al-Aqtash, N., & Sabirianov, R. F. (2016). Band gap modulation in polythiophene and polypyrrole-based systems. Scientific Reports, 6, 36554.
8. Namsheer, K., & Rout, C. S. (2021). Conducting polymers: A comprehensive review on recent advances in synthesis, properties and applications. RSC Advances, 11(10), 5659–5697.
9. Wang, Y., Chen, L., & Zhang, H. (2023). Acid vapor doping of polar polythiophenes for high electrical conductivity. Journal of Materials Chemistry C, 11(30), 10218–10227.
10. Yu, X., Zhou, G., Zhang, J., & Yang, X. (2016). Highly conductive polythiophene films doped with chloroauric acid for dual-mode sensing. Sensors and Actuators B: Chemical, 238, 204–213.
11. Zhao, K., Khan, H. U., Li, R., Su, Y., & Amassian, A. (2017). Entanglement of conjugated polymer chains influences molecular self-assembly and carrier transport. Advanced Functional Materials, 27(19), 1605908.
12. Bao, Q., Liu, X., Braun, S., & Fahlman, M. (2015). Oxygen- and water-based degradation in conjugated polymers. Advanced Energy Materials, 5(6), 1401442.
13. Gao, J., Roehling, J. D., Li, Y., Guo, H., Moulé, A. J., & Grey, J. K. (2016). The effect of doping on the microstructure and charge transport of P3HT films. Journal of Materials Chemistry C, 4(15), 3112–3121.
14. Patel, S. N., Glaudell, A. M., Peterson, K. A., Thomas, E. M., O'Hara, K. A., Lim, E., & Chabinyc, M. L. (2017). Morphology controls the thermoelectric power factor of a doped semiconducting polymer. Science Advances, 3(6), e1700434.
15. Thomas, E. M., Peterson, K. A., Balzer, A. H., Rawlings, D., Stingelin, N., Segalman, R. A., & Chabinyc, M. L. (2020). Effects of counter-ion size on delocalization and conductivity in doped semiconducting polymers. Advanced Electronic Materials, 6(12), 2000595.
16. Hamidi-Sakr, A., Biniek, L., Bantignies, J.-L., Maurin, D., Herrmann, L., Leclerc, N., & Brinkmann, M. (2017). A versatile method to fabricate highly in-plane aligned conducting polymer films. Advanced Functional Materials, 27(25), 1700173.
17. Kroon, R., Mengistie, D. A., Kiefer, D., Hynynen, J., Ryan, J. D., Yu, L., & Müller, C. (2016). Thermoelectric plastics: From design to synthesis, processing and structure–property relationships. Chemical Society Reviews, 45(22), 6147–6164.